Eur. Phys. J. B **56**, 273–278 (2007)
DOI: 10.1140/epjb/e2007-00114-7

THE EUROPEAN PHYSICAL JOURNAL B

Excitable scale free networks

M. Copelli[1,a] and P.R.A. Campos[2,b]

[1] Laboratório de Física Teórica e Computacional, Departamento de Física, Universidade Federal de Pernambuco, 50670-901 Recife, PE, Brazil
[2] Departamento de Física, Universidade Federal Rural de Pernambuco, 52171-900 Recife, PE, Brazil

Received 29 November 2006 / Received in final form 30 March 2007
Published online 4 May 2007 –

Abstract. When a simple excitable system is continuously stimulated by a Poissonian external source, the response function (mean activity versus stimulus rate) generally shows a linear saturating shape. This is experimentally verified in some classes of sensory neurons, which accordingly present a small dynamic range (defined as the interval of stimulus intensity which can be appropriately coded by the mean activity of the excitable element), usually about one or two decades only. The brain, on the other hand, can handle a significantly broader range of stimulus intensity, and a collective phenomenon involving the interaction among excitable neurons has been suggested to account for the enhancement of the dynamic range. Since the role of the pattern of such interactions is still unclear, here we investigate the performance of a scale-free (SF) network topology in this dynamic range problem. Specifically, we study the transfer function of disordered SF networks of excitable Greenberg-Hastings cellular automata. We observe that the dynamic range is maximum when the coupling among the elements is critical, corroborating a general reasoning recently proposed. Although the maximum dynamic range yielded by general SF networks is slightly worse than that of random networks, for special SF networks which lack loops the enhancement of the dynamic range can be dramatic, reaching nearly five decades. In order to understand the role of loops on the transfer function we propose a simple model in which the density of loops in the network can be gradually increased, and show that this is accompanied by a gradual decrease of dynamic range.

PACS. 87.19.La Neuroscience – 87.18.Sn Neural networks – 89.75.Hc Networks and genealogical trees 89.20.-a Interdisciplinary applications of physics

1 Introduction

Recent applications of tools from Statistical Physics have brought about new perspectives to theoretical Neuroscience. On the one hand, networks of simplified neuron models seem to capture essential features of collective neuronal dynamics [1–5], very often being also amenable to analytical calculations via mean field approximations or Fokker-Planck equations [6–8]. On the other hand, experimental data from real neural networks have yielded extremely interesting results when analyzed within the framework of complex networks, often revealing the small-world character for structural (i.e. anatomical) connectivity in different spatial scales [9–11], as well as scale-free characteristics for functional connectivity both in in vitro [12] and in fMRI [13,14] data (see [15] for a recent review).

In the context of modelling, one intriguing question in Neuroscience regards the stunning ability that brains have to cope with sensory stimuli that vary over many orders of magnitude [7]. The experimental evidence supporting this claim has been accumulating for about a century in the Psychophysics literature: the perception of a given stimulus grows with a power law of the stimulus intensity (Stevens law), with an exponent (Stevens exponent) which is typically <1, implying low-stimulus amplification and large dynamic range [16]. This is in stark contrast with the poor performance of single neurons: as a function of the stimulus intensity, the mean firing rate of sensory neurons experimentally shows the linear saturating shape that one expects for general excitable systems, so their responses consistently have a small dynamic range, typically about one or two decades only [17–20]. How can these two experimental results be reconciled? A solution which has been proposed for this apparent paradox involves a collective phenomenon. The idea is that if excitable elements with small dynamic range are coupled, signal propagation in the network amplifies the average activity, as compared to that of an isolated node. This collectively leads to a significant enhancement of dynamic range, thus providing a possible solution to a problem faced by biological as well as artificial sensors: how to code for several orders of magnitude of stimulus intensity, starting from narrow-coding elements [2–4,6,7].

[a] e-mail: mcopelli@df.ufpe.br
[b] e-mail: paulo.campos@df.ufrpe.br

The reasoning underlying the enhancement of dynamic range is very general and applies to essentially any network topology. Consider the limit of very weak stimulus, where each excitable element has a small probability of being excited. By coupling the elements, a single stimulus event will be amplified to neighboring sites, which will further amplify it, and so forth. If the coupling strength is small, this excitable wave will eventually die out, but the overall network activity (the response to the stimulus) will still be larger than that of the isolated element that originally received the stimulus. The larger the coupling strength, the larger the amplification, and so the sensitivity and the dynamic range of the response curve initially increase with coupling. There is, however, a critical value of the coupling above which self-sustained activity becomes stable. Above this (typically second order) nonequilibrium phase transition, the response of the network for weak stimulus is hindered, because it is masked by the self-sustained activity of the network. This gets worse and worse as the coupling increases, so above criticality the dynamic range of the response curve decreases with increasing coupling strength. Therefore, the dynamic range is optimal at criticality [7].

The above mechanism has been tested in regular [2–4,6] as well as random [7] networks of excitable elements. The maximum enhancement in dynamic range is about 100% in one-dimensional networks [6] and 50% in random graphs [7]. It is not a priori clear how the performance depends on the network topology and, in particular, which one gives the best results. Given the potential applications of the mechanism to artificial sensors, as well as the relevance to Neuroscience, in this paper we study the performance of a scale-free topology in the dynamic range problem. We show that a particular class of scale-free networks, those with no loops, yield the best performance known so far. We investigate the role of loops on the dynamic range by introducing a slightly modified version of the Barabási-Albert scale-free model where we can now tune the amount of loops in the network.

The paper is organized as follows. In Section 2 we introduce the model and give a precise definition of the dynamic range. Results are discussed in Section 3 for the standard Barabási-Albert scale-free model (3.1) as well as for a slightly modified "loop-diluted" version that we introduce (3.2). Our concluding remarks are presented in Section 4.

2 The model

We consider a variant of the Greenberg-Hastings cellular automaton [21], which is one of the simplest models of an excitable system and can be used in large-scale simulations. In the model, each excitable node $i = 1, \ldots, N$ could represent either a neuron, an active dendritic patch or even sub-cellular excitable processes. Each node can be in one of n states: $x_i = 0$ is the quiescent state (e.g. a polarized neuron), $x_i = 1$ is the excited state (e.g. a spiking neuron) and $x_i = 2, \ldots, n-1$ are refractory states (e.g. a hyperpolarized neuron). Once a site is excited ($x_i = 1$), it deterministically goes through the next $n-2$ refractory states, after which it jumps to the quiescent state $x_i = 0$ (the automaton is therefore cyclic [22]). Each node is independently excited by a stochastic external source, which mimics the effect of an stimulus on the lattice. We model the arrival of a suprathreshold stimulus by a Poisson process with rate r: at each time step τ an attempt to stimulate a site occurs with probability

$$\lambda = 1 - \exp(-r\tau) \tag{1}$$

(we adopt the arbitrary time scale of $\tau = 1$ ms, which is the characteristic time scale of a neuronal spike). We refer to the rate r as the stimulus intensity. In order to become excited in time $t + \tau$ a given site has to be in state 0 at time t. There are two different ways by which a site can be excited: by the continuous stimulation of the external source (with probability λ per time step) or by stimulus propagation from its excited neighbors. Thus the probability that a quiescent site i is excited in the next time step is

$$P_i(t+\tau) = 1 - (1-\lambda)\prod_{j=1}^{k_i}(1 - p_{ij})\delta(x_j(t), 1), \tag{2}$$

where $\delta(a, b)$ is the Kronecker delta, k_i is the number of neighbors (connectivity or degree) of site i and p_{ij} is the probability that excitation from site j gets transmitted to site i. There is quenched disorder in the coupling: the probabilities p_{ij} are initially drawn from a uniform distribution in $[0, 2\sigma/K]$ if $2\sigma/K < 1$, or $[2\sigma/K - 1, 1]$ if $2\sigma/K > 1$, where $K = \langle k \rangle$ is the mean connectivity of the network and σ is the coupling parameter (for simplicity, we consider the case of bidirectional coupling $p_{ij} = p_{ji}$). Note that, in a mean field approximation, σ coincides with the branching ratio, defined as the average of the number of descendant excitations divided by the number of ancestor excitations of each site. Such mean field approximation provides a quite satisfactory agreement with simulation results for random graph topologies (as expected) and accurately predicts a phase transition at $\sigma_c = 1$ [5,7].

The mean firing rate of the network is defined as $F \equiv T^{-1}\sum_t^T \rho_t$, where $\rho_t \equiv N^{-1}\sum_i^N \delta(x_i(t), 1)$ is the instantaneous density of active (excited) sites and T is a given time window for measurements (we have used $N = 10^4$, $T = 10^4$ steps and $n = 5$ states in most simulations). We refer to $F(r)$ as the *response function* (or transfer function) of the network. It typically shows the sigmoidal shape in a log-linear scale exemplified in Figure 1a, with a baseline activity $F_0 \equiv \lim_{r\to 0} F(r)$ and saturation at $F_{max} \equiv \lim_{r\to\infty} F(r)$. The dynamic range Δ of the response function is defined as the width (measured in dB) in stimulus intensity r which can be "appropriately coded" by F. In the biological literature, this is usually operationalized as follows [17,18]: by letting $F_x \equiv F_0 + x(F_{max} - F_0)$, where $0 \le x \le 1$, and r_x be the corresponding stimulus intensity, ($F(r_x) = F_x$, see triangles in Fig. 1a for an example), the dynamic range is defined as

$$\Delta = 10\log_{10}\left(\frac{r_{0.9}}{r_{0.1}}\right), \tag{3}$$

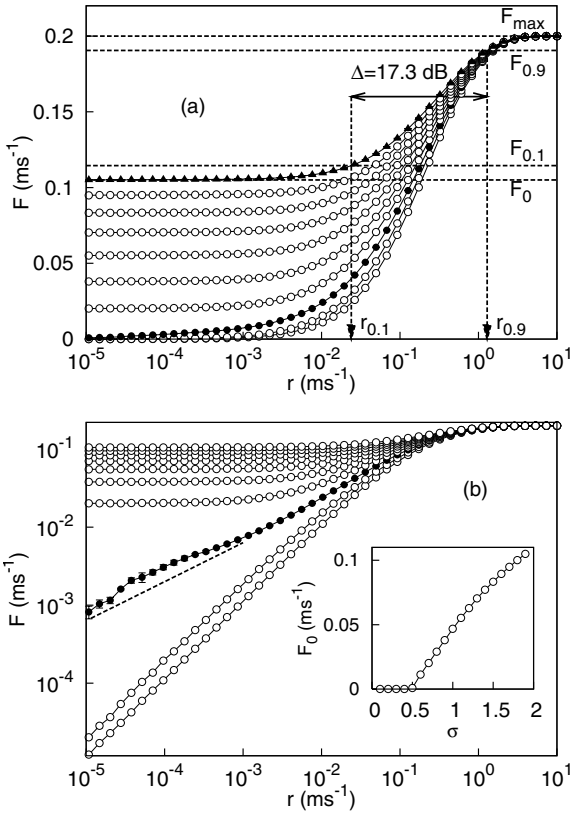

Fig. 1. (a) Response functions for BA scale-free networks with $m = 10$: mean firing rate F versus stimulus rate r. Different curves denote different values of the branching parameter σ: from bottom to top, $\sigma = 0.1, 0.3, \ldots, 1.9$. Filled circles: $\sigma = 0.5$, which is close to the critical value. The horizontal lines exemplify how the dynamic range Δ is calculated for $\sigma = 1.9$ (filled triangles). (b) Log-log version of (a). The dashed line shows an exponent 1/2. Inset: self-sustained activity F_0 versus σ, illustrating the phase transition close to $\sigma_c \simeq 0.5$.

therefore excluding stimuli whose response is just above baseline ($r < r_{0.1}$) or too close to saturation ($r > r_{0.9}$). For an isolated Greenberg-Hastings excitable node, one can easily show that the dynamic range is $\Delta \lesssim 19$ dB [4,6].

3 Results

3.1 Barabási-Albert networks

We consider scale-free networks [23] of such excitable elements. Several investigations show that distinct systems such as World-Wide Web [23], scientific [24], metapopulation dynamics [25,26] and biochemical networks [27,28] self-organize into a scale-free configuration [29], which means that the probability P_k that a given node has k edges follows a power-law distribution like

$$P_k \propto k^{-\gamma}. \tag{4}$$

Measurements in real systems estimate γ in the range $[2, 3]$. Equation (4) basically means that poorly-connected nodes are most frequent in the network than well-connected nodes (hubs).

To establish scale-free networks, we follow the standard algorithm by Barabási and Albert (BA) [23], which regards preferential attachment and growth as mechanisms for the emergence of the scale-free character. In this algorithm, the resulting networks display connectivity distribution according to $P_k \propto k^{-3}$. The parameters of the BA model are the number of nodes N and m, which corresponds to the number of links that a newly introduced node adds to the network. These m links are most probably attached to those nodes with an already large number of edges.

Figure 1 shows the results for $m = 10$. For small values of σ, the response function $F(r)$ increases linearly for weak stimulus. This linearity can be easily interpreted: each stimulus arrival generates an excitable wave that will have a finite lifetime and will die before another wave is created. For stronger stimulus (larger r) linearity breaks down, since there is interaction among waves, which partially annihilate each other. For very large r, the firing rates reach a saturation value which scales with the inverse of the refractory period, $F_{max} = 1/n$ [2–4]. As the value of σ increases, so does the lifetime of an excitable wave, leading to larger amplification of weak stimuli and a corresponding enhancement of dynamic range (see Fig. 2 for $\sigma \lesssim 0.5$). When $\sigma = \sigma_c$, the lifetime of the excitable waves effectively diverges and the system undergoes a second order phase transition (notice the change in the exponent in the filled circles of Fig. 1b). For $\sigma > \sigma_c$, any perturbation in the network will lead to a stable self sustained activity, $F_0 > 0$ (inset of Fig. 1b) which, as explained in section 1, leads to smaller values of the dynamic range as the coupling increases [7] (see Fig. 2 for $\sigma \gtrsim 0.5$).

One observes that, differently from random graph topologies [7], the transition for scale-free excitable networks occurs at $\sigma_c < 1$. We speculate that this is due to the hubs, which have a local branching ratio $\sigma_i = \sum_j^{k_i} p_{ij}$ larger than unit even for $\sigma < 1$ and could therefore facilitate the transition. It is also interesting to note that deviations from mean field behavior have been predicted for the contact process (CP) in a scale-free network [30]. Apart from the refractory period and the disorder, the CP is similar to the model we study here (in the sense that it has a unique absorbing state with no symmetries). In Fig. 1, however, the response exponent at criticality (defined by $F(r; \sigma_c) \sim r^{1/\delta_h}$) seems to be compatible with the mean field value $1/\delta_h = 1/2$ [22].

Results in Figure 1 are typical, similar curves are obtained for any $m > 1$. The performance of these scale-free networks in enhancing the dynamic range is poor: while the dynamic range of isolated excitable elements is $\Delta(\sigma = 0) \simeq 16.7$ dB, the network (optimal) performance at criticality is only $\Delta(\sigma_c) \simeq 20.8$ dB, an enhancement of less than a decade. This is slightly worse than the enhancement produced by random networks with equivalent size and average connectivity, as can be seen in the curves $\Delta(\sigma)$ of Figure 2.

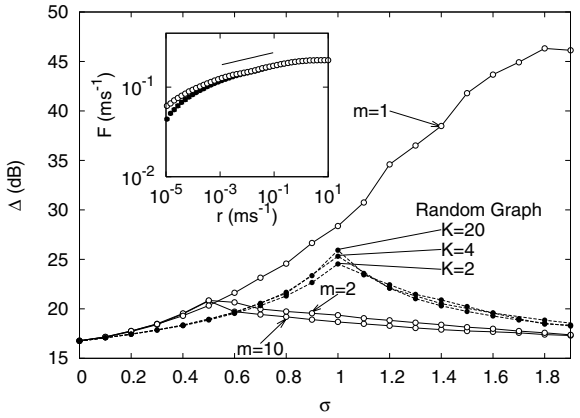

Fig. 2. Dynamic range Δ versus branching parameter σ for distinct network topologies: BA scale-free networks (open circles) and Erdős-Rényi random graphs (filled circles) with approximately the same mean connectivity. Inset: Response function for BA scale-free networks with $m = 1$ and $\sigma = 2$ for $N = 10^4$ (filled circles) and $N = 3 \times 10^4$ (open circles). The solid line shows a slope $\simeq$0.07.

The case $m = 1$, however, is particularly interesting. Notice that in this situation the network is still scale-free, but does not comprise any loop in its structure and consequently has a tree-like pattern. This condition, together with the deterministic nature of each excitable node after excitation, prevents the phase transition to self-sustained activity from occurring [1], a fact that has also been observed in one-dimensional excitable networks [6]. In these conditions the only transition occurs at $\sigma = \sigma_{max} = K$ ($=2m$ for scale-free networks), whereby propagation of excitable waves becomes deterministic (ballistic). Therefore low-stimulus amplification increases steadily with σ, but in the absence of self-sustained activity ($F_0 = 0$). This allows the dynamic range to increase monotonically with σ, reaching values near 50 dB, which is the largest value obtained so far in excitable network models.

3.2 Loop-diluted model

As we observe a remarkable difference between the dynamic range of scale-free networks with $m = 1$ and other values of m, and the former has a typical feature (nonexistence of loops) which is not present in $m > 1$ topologies, we are interested in investigating the role of loops in the response functions of the networks. For this purpose, we propose a variant of the BA model which is referred to as loop-diluted model. In the model each new node is added according to the usual preferential attachment rule, but can have $m = 1$ or $m = 2$ links according to the probability distribution

$$P(m) = (1 - p)\delta_{m,1} + p\delta_{m,2}, \qquad (5)$$

where p is the probability of having two edges. So p adjusts the amount of loops in the network and the case $p = 0$ recovers the structure with no loops. The mean degree is now $K = 2\langle m \rangle = 2(1 + p)$.

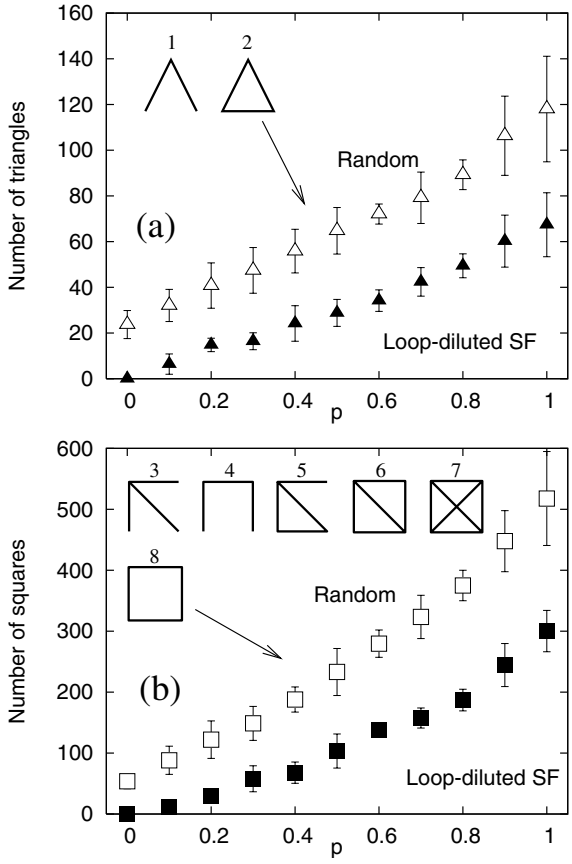

Fig. 3. Occurrences of 3- and 4-site patterns in the loop-diluted scale-free networks (filled symbols) and their randomized counterparts (open symbols). (a) number of triangles versus p and (b) number of squares versus p. Points (bars) represent the mean (standard deviation) over 5 realizations for $N = 1000$. Patterns are sequentially numbered (1–8) for further reference in the text.

Notice that, since all sites belong to a single giant component, the average number of loops created by each newly added site is bounded from below by p. Each new two-edged node can give rise to loops of any size, but the relationship between parameter p and the number of loops becomes already apparent in a simple 3-site motif analysis [31]. Figure 3a shows the mean number of triangles as a function of p (calculated by the free software available at `www.weizman.ac.il/mcb/UriAlon`). As expected, this is a monotonically increasing function, which nevertheless stays well below Np, hinting that most loops comprise more than three sites. The same qualitative scenario is observed when we plot the number of squares (Fig. 3b), which are more abundant than triangles. In both cases, we notice that for equally sized randomized graphs (which preserve the degrees of every node [31]), the numbers of triangles and squares are considerably larger. This means that triangles and squares are actually *anti-motifs* in the loop-diluted model [32]. In fact, this is true for all patterns that contain loops (numbered 2, 5, 6 and 8 in Fig. 3), except for pattern 7, which cannot occur according to the growth rules of the model. The occurrences of patterns 1,

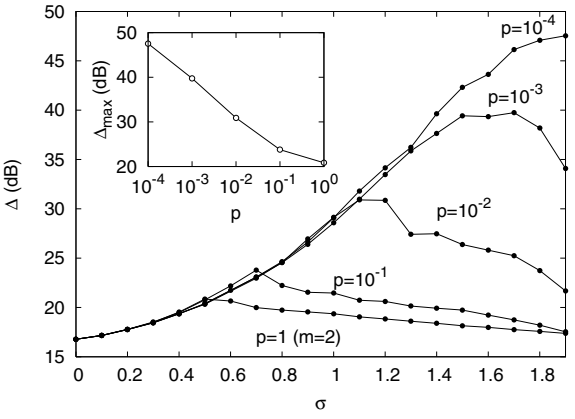

Fig. 4. Dynamic range Δ versus branching parameter σ for the loop-diluted model and different values of the probability p that a newly added node has two incoming edges. Inset: maximum value of the dynamic range as a function of p.

3 and 4 in the loop-diluted model and in the randomized networks are statistically indistinguishable (therefore they are neither motifs nor anti-motifs — data not shown).

Figure 4 displays the dynamic range Δ as a function of the coupling σ for some values of p. From the figure, we clearly notice that the insertion of loops by increasing the probability p has a striking effect on the dynamic range. This effect is already mensurable for values of p such that $pN \sim 1$. The peak value of the dynamic range $\Delta_{max}(p) \equiv \max_\sigma \Delta(\sigma; p) = \Delta(\sigma_c(p); p)$ seems to decrease logarithmically with p.

4 Concluding remarks

Recently, some investigations have addressed the enlargement in average activity of excitable elements by coupling these entities and so giving form to a new larger and more sensitive unit. Although this collective phenomenon has been widely accepted, little is known about the way the arrangement of connections among the excitable elements acts physically on the system dynamics. The creation of more robust and functional units from smaller units (whose pattern of interactions is a determining aspect) is of course not exclusive of Neuroscience. For instance, the hypercycle, a catalytic feedback network whereby each element helps the replication of the next one in a regulatory cycle closing on itself, has been pondered as an alternative resolution for the information crisis in prebiotic evolution [33,34]. We believe that all the recent contributions on this issue have a bearing on a more general context, that is, the understanding of the interplay between system dynamics and the underlying interaction network topologies. We hope that our contribution gives a small step in this direction, when we corroborate that the amount of loops in network structure could be a key topological feature.

We have presented simulation results for the transfer function of excitable scale-free networks. The behavior of the dynamic range Δ as a function of the coupling σ shows the general behavior predicted in reference [7]: in the subcritical regime ($\sigma < \sigma_c$) $\Delta(\sigma)$ increases, while in the supercritical regime ($\sigma > \sigma_c$) $\Delta(\sigma)$ decreases. The maximum value is obtained at criticality, but for scale-free networks with $m > 1$ this result is even smaller than that for a random graph.

For $m = 1$ the phase transition to self-sustained activity disappears, and the dynamic range increases steadily, reaching its maximum value when excitable waves become deterministic. This suggests that the presence of loops in the network could be a relevant feature in determining the dynamic range of its transfer function. We have introduced a simple extension to the BA scale-free model which allows one to interpolate between $m = 1$ and $m = 2$, showing that dynamic range decreases as the density of loops increases. This reinforces the need to study other topologies with tree structure, which abound in biological structures.

It remains at present unclear whether the response exponent for $m > 1$ is indeed compatible with the mean field universality class (even though this seems to be supported by recent simulation results in reference [35], which independently addressed a similar problem). Also, for $m = 1$ at maximum coupling, the response function seems to be governed by a power law with a much smaller exponent (see inset of Fig. 2) which might not belong to the directed percolation universality class. We believe that a detailed study of the critical exponents of excitable scale-free networks is still lacking and should be dealt with in the future.

M.C. and P.R.A.C. are supported by Conselho Nacional de Desenvolvimento Científico e Tecnológico (CNPq), FACEPE and special program PRONEX.

References

1. T.J. Lewis, J. Rinzel, Network: Comput. Neural Syst. **11**, 299 (2000)
2. M. Copelli, A.C. Roque, R.F. Oliveira, O. Kinouchi, Phys. Rev. E **65**, 060901 (2002)
3. M. Copelli, R.F. Oliveira, A.C. Roque, O. Kinouchi, Neurocomputing **65-66**, 691 (2005)
4. M. Copelli, O. Kinouchi, Physica A **349**, 431 (2005)
5. C. Haldeman, J.M. Beggs, Phys. Rev. Lett. **94**, 058101 (2005)
6. L.S. Furtado, M. Copelli, Phys. Rev. E **73**, 011907 (2006)
7. O. Kinouchi, M. Copelli, Nat. Phys. **2**, 348 (2006)
8. B. Doiron, J. Rinzel, A. Reyes, Phys. Rev. E **74**, 030903 (2006)
9. D.J. Watts, S.H. Strogatz, Nature **393**, 440 (1998)
10. L.A.N. Amaral, A. Scala, M. Barthélémy, H.E. Stanley, PNAS **97**, 11149 (2000)
11. S. Sakata, Y. Komatsu, T. Yamamori, Neurosci. Res. **51**, 309 (2005)
12. J.M. Beggs, D. Plenz, J. Neurosci. **23**, 11167 (2003)
13. V.M. Eguíluz, D.R. Chialvo, G.A. Cecchi, M. Baliki, A.V. Apkarian, Phys. Rev. Lett. **94**, 018102 (2005)

14. D.R. Chialvo, Physica A **340**, 756 (2004)
15. O. Sporns, D.R. Chialvo, M. Kaiser, C.C. Hilgetag, Trends Cog. Sci. **8**, 418 (2004)
16. S.S. Stevens, *Psychophysics: Introduction to its Perceptual, Neural and Social Prospects* (Wiley, New York, 1975)
17. S. Firestein, C. Picco, A. Menini, J. Physiol. **468**, 1 (1993)
18. J.-P. Rospars, P. Lánský, P. Duchamp-Viret, A. Duchamp, BioSystems **58**, 133 (2000)
19. J.-P. Rospars, P. Lánský, P. Duchamp-Viret, A. Duchamp, Eur. J. Neurosci. **18**, 1135 (2003)
20. M.R. Deans, B. Volgyi, D.A. Goodenough, S.A. Bloomfield, D.L. Paul, Neuron **36**, 703 (2002)
21. J.M. Greenberg, S.P. Hastings, SIAM J. Appl. Math. **34**, 515 (1978)
22. J. Marro, R. Dickman, *Nonequilibrium Phase Transition in Lattice Models* (Cambridge University Press, Cambridge, 1999)
23. A.-L. Barabási, R. Albert, Science **286**, 509 (1999)
24. M.E.J. Newman, Proc. Natl. Acad. Sci. **98**, 404 (2001)
25. Y. Moreno, R. Pastor-Satorras, A. Vespignani, Eur. Phys. J. B **26**, 521 (2002)
26. V. Vuorinen, M. Peltomäki, M. Rost, M.J. Alava, Eur. Phys. J. B **38**, 261 (2004)
27. H. Jeong, B. Tombor, R. Albert, Z.N. Oltvai, A.-L. Barabási, Nature **407**, 651 (2000)
28. H. Jeong, S.P. Mason, A.-L. Barabási, Z.N. Oltvai, Nature **411**, 41 (2001)
29. R. Albert, A.-L. Barabási, Rev. Mod. Phys. **74**, 47 (2002)
30. C. Castellano, R. Pastor-Satorras, Phys. Rev. Lett. **96**, 038701 (2006)
31. R. Milo, S. Shen-Orr, S. Itzkovitz, N. Kashtan, D. Chklovskii, U. Alon, Science **298**, 824 (2002)
32. R. Milo, S. Itzkovitz, N. Kashtan, R. Levitt, S. Shen-Orr, I. Ayzenshtat, M. Sheffer, U. Alon, Science **303**, 1538 (2004)
33. M. Eigen, S.P. Naturwissenschaften **65**, 7 (1978)
34. P.R.A. Campos, J.F. Fontanari, P.F. Stadler, Phys. Rev. E **61**, 2996 (2000)
35. A.-C. Wu, X.-J. Xu, Y.-H. Wang, Phys. Rev. E **75**, 032901 (2007)